1 # Disentangling metabolic functions of bacteria in the

2 # honey bee gut

3

4 Lucie Kešnerová[1,#], Ruben A. T. Mars[2,#], Kirsten M. Ellegaard[1], Michaël Troilo[1],

5 Uwe Sauer[2], Philipp Engel[1]*

6

7 [1]Department of Fundamental Microbiology, University of Lausanne, 1015

8 Lausanne, Switzerland

9 [2]Institute of Molecular Systems Biology, ETH Zürich, 8093 Zürich, Switzerland

10

11 ***Correspondence:**

12 Prof. Philipp Engel

13 Department of Fundamental Microbiology

14 University of Lausanne, CH-1015 Lausanne, Switzerland

15 Tel.: +41 (0)21 692 56 12

16 e-mail: philipp.engel@unil.ch

17

18 [#]L.K and R.A.T.M. contributed equally to this work.

19

20 **Short title:** Honey bee gut microbiota metabolomics

21

22

23

24

Abstract

It is presently unclear how much individual community members contribute to the overall metabolic output of a gut microbiota. To address this question, we used the honey bee, which harbors a relatively simple and remarkably conserved gut microbiota with striking parallels to the mammalian system and importance for bee health. Using untargeted metabolomics, we profiled metabolic changes in gnotobiotic bees that were colonized with the complete microbiota reconstituted from cultured strains. We then determined the contribution of individual community members in mono-colonized bees, and recapitulated our findings using *in vitro* cultures. Our results show that the honey bee gut microbiota utilizes a wide range of pollen-derived substrates including flavonoids and outer pollen wall components, suggesting a key role for degradation of recalcitrant secondary plant metabolites and pollen digestion. In turn, multiple species were responsible for the accumulation of organic acids and polyphenol degradation products, and a specific gut symbiont, *Bifidobacterium asteroides,* stimulated the production of host hormones known to impact bee development. While we found evidence for cross-feeding interactions, ~80% of the identified metabolic changes were also observed in mono-colonized bees with *Lactobacilli* being responsible for the largest share of the metabolic output. These results suggest that bacteria in the honey bee gut colonize largely independent metabolic niches, which may be a general characteristic of gut microbiomes. Our study reveals diverse metabolic functions of gut bacteria that are likely to contribute to bee health, and provide fundamental insights into how metabolic functions are partitioned within gut communities.

Author summary

Honey bees are important pollinators that harbor a simple gut microbiota with striking parallels to the mammalian system. This makes them relevant models to study gut microbiota functions and its impact on host health. We applied untargeted metabolomics to characterize metabolic changes induced by the gut microbiota, and to characterize contributions of the major community members. We find that the gut microbiota digests recalcitrant substrates derived from the bees' pollen-diet. Most metabolic changes could be explained by the activity of individual community members suggesting substrate specificity and independent metabolic niches. Our study provides novel insights into the functional understanding of the bee gut microbiota and provides a framework for applying untargeted metabolomics to disentangle metabolic functions of gut bacteria.

Introduction

Metabolic activities of the microbiota are key for establishing mutualistic interactions in the gut and thereby affect the host in conditions of health and disease. Gut bacteria facilitate the breakdown of refractory or toxic dietary compounds [1-3], produce metabolites that promote host growth and physiology [4-7], and modulate immune functions in the gut [8] and other tissues [9,10]. Moreover, metabolic activity is the basis for energy and biomass production resulting in bacterial growth and the occupation of ecological niches conferring colonization resistance against pathogenic microbes [11]. Substrates of gut bacteria predominantly originate from the diet of the host [2,12], making diet the major modulator of the composition and metabolic activity of the gut microbiota [13,14].

The substantial metabolic potential of the animal gut microbiota has been profiled by the direct sequencing of functional gene content (i.e. shotgun metagenomics) [15-18]. However, it is challenging to predict functional metabolic output from such sequencing data. With recent advances in the coverage and throughput of untargeted screening metabolomics [19-21], it has become feasible to quantify metabolic changes in microbiota or host tissues at large coverage and throughput. Besides identifying metabolites connected to human health and disease [22-30], untargeted screening metabolomics holds considerable promise to unravel metabolic functions of individual microbiota members in animals with divergent dietary preferences. Such mono-colonization studies are however complicated by the highly variable and species-rich composition of most animal microbiota. Thus, gut communities of reduced

87 complexity are valuable models to disentangle metabolic functions of the
88 constituent species.

89   Like mammals, honey bees harbor a highly specialized gut microbiota.
90 However, the honey bee gut microbiota is surprisingly simple and conserved
91 with seven species (categorized by clustering at 97% 16S rRNA sequence
92 identity) accounting for >90% of the entire gut community in bees sampled
93 across continents [31]. This microbiota is composed of four Proteobacteria
94 (*Gilliamella apicola, Snodgrassella alvi, Frischella perrara*, *Bartonella apis*), which
95 mostly reside in the ileum, and two Firmicutes (*Lactobacillus* spp. Firm-4 and
96 Firm-5) and one Actinobacterium *(Bifidobacterium asteroides*), which are
97 predominantly found in the rectum. These specific locations suggest that
98 bacteria occupy different metabolic niches in the bee gut and potentially engage
99 in syntrophic interactions [32,33].

100   The honey bee gut microbiota has marked effects on the host. It promotes
101 host weight gain and hormone signaling under laboratory setting [34] and
102 stimulates the immune system of the host [35,36]. In addition, honey bees are
103 ecologically and economically essential pollinators that have experienced
104 increased mortality in recent years [37,38], which could in part be due to
105 disturbances of their microbiota composition [39-42].

106   Genomic analyses in combination with *in vitro* cultures have shown that
107 fermentation of sugars and complex carbohydrates (e.g. pectin) [15,32,43,44]
108 into fermentation products is the dominant metabolic activity of the gut
109 microbiota [34]. Lacking however is a detailed understanding of the
110 consumption of diet-derived substrates and how individual community
111 members contribute to the metabolic activities *in vivo*. It is for instance elusive

112   whether analogously to mammals recalcitrant dietary compounds (especially

113   from pollen) are broken down by the microbiota in the hindgut (i.e. large

114   intestine composed of ileum and rectum), while more accessible compounds are

115   reportedly absorbed by the host in the midgut (i.e. small intestine) [45-47].

116   To profile the metabolic output of the honey bee gut microbiota and its

117   individual members, we employed gnotobiotic bee colonizations and *in vitro*

118   experiments in conjunction with untargeted metabolomics **(Figure 1)**. We first

119   characterized robust metabolic differences between microbiota-free bees and

120   bees colonized with a reconstituted community composed of the seven major

121   bacterial species of the gut microbiota. Subsequently, we analyzed bees

122   colonized with each community member separately to assay their potential

123   contribution to the overall metabolic output of the gut microbiota. Finally, we

124   recapitulated our results *in vitro* using pollen-conditioned medium. Our

125   systematic approach provides unprecedented insights into the metabolic

126   activities of the honey bee gut microbiota and demonstrates the usefulness of

127   metabolomics in combination with gnotobiotic animal models to disentangle

128   functions of individual gut microbiota members.

129

Results and Discussion

Experimental reconstitution of the honey bee gut microbiota.

To characterize the metabolic output of the honey bee gut microbiota, we colonized microbiota-free (MF) bees with selected bacterial strains previously isolated from the bee gut. The reconstituted bacterial community consisted of eleven strains **(Table S1)** covering the seven species described above. We used two strains for *G. apicola* and four strains for Firm-5 in order to cover the extensive genetic diversity within these species [44,48]. Exposure of MF bees to this community resulted in the successful establishment of all seven species with a total of $10^9 - 10^{10}$ bacterial cells per gut after 10 days of colonization (**Figure 2, Figure S1A**). In contrast, non-colonized MF bees had bacterial levels <10^5 per gut, an observation consistent with previous studies [32,49]. Compared to hive bees of the same age, bacterial abundances of most species were slightly elevated in colonized (CL) bees. However, in both groups the Firm-5 species was consistently the most abundant community member, while *B. apis* colonized at much lower levels. This is in line with recent 16S rRNA gene-based community analysis [31,50,51], and we thus conclude that the selected strains assembled into a structured community resembling the native honey bee gut microbiota. This validates our gnotobiotic bee system as a tool for microbiota reconstitution experiments and enables the study of microbiota functions under controlled laboratory conditions.

152 **Metabolic changes in the honey bee gut upon colonization with the**

153 **reconstituted bacterial community.**

154 To reveal microbiota-induced metabolome changes in the gut, we dissected the

155 combined mid- and hindgut of MF, CL and hive bees and analyzed water-

156 extracted homogenates of these gut samples by untargeted metabolomics [21].

157 In total, we detected 24,899 mass-to-charge features (ions), 1,079 of which could

158 be annotated by matching their accurate mass to sum formulas of compounds in

159 the full KEGG database (**Dataset S1**). These 1,079 ions putatively correspond to

160 3,270 metabolites, since this method cannot separate isobaric compounds

161 (**Supplemental methods**). For ion changes with multiple annotations, we

162 provided the most likely annotation as based on information from literature and

163 genomic data.

164 Principal component analysis on the ion intensities revealed that CL and

165 MF bees separate into two distinct clusters suggesting colonization-specific

166 metabolic profiles (**Figure S1B**). In two independent experiments, a total of 372

167 ions exhibited significant changes between CL and MF bees (Welch's t-test, BH

168 adj. P ≤0.01). A subset of 240 ions (65%) were more abundant in MF bees

169 suggesting that the cognate metabolites are utilized by the gut microbiota. These

170 ions are hereafter referred to as bacterial substrates. Conversely, 132 ions were

171 more abundant in CL bees and are hereafter referred to as bacterial products

172 indicating that they are produced either by the microbiota or by the host in

173 response to the microbiota. To facilitate the biological interpretation of these

174 multitude metabolic changes, we carried out two analyses. First, we looked

175 whether certain compound classes were overrepresented among the subsets of

176 bacterial substrates and products (**Dataset S2**). Second, we sorted ion changes

177 based on their ability to explain the difference between the MF and CL

178 metabolome profiles in an Orthogonal Projection of Least Squares-

179 Differentiation Analysis (OPLS-DA) [52] **(Figure 3)**.

180

181 **Major bee gut microbiota substrate classes**.

182 We first focused on the 240 substrate ions that were more abundant in MF vs CL

183 bees to reveal metabolites potentially utilized by the microbiota. We found three

184 compound classes to be strongly enriched: *flavonoids* (20 of 36 annotated ions,

185 one-sided Fisher's exact test, *P* <0.001), and both *purine-* and *pyrimidine*

186 *nucleosides* (in total 8 of 9 annotated ions, both *P* <0.01)**.** Seven flavonoids, three

187 nucleosides, and a nucleoside precursor (orotate, *m/z* 155.009) were also among

188 the 28 substrate ions with most discriminatory power for distinguishing CL vs

189 MF bees as based on OPLS-DA (**Figure 3**). Other ions among these most

190 discriminatory substrates included two ω-hydroxy acids (*m/z* 315.254 and *m/z*

191 331.249) and three phenolamides (*m/z* 582.260, *m/z* 630.245, *m/z* 233.130)

192 from the outer pollen wall, as well as quinate (*m/z* 191.056), and citrate (*m/z*

193 191.019), both of which had previously been predicted to be utilized by certain

194 community members of the honey bee gut microbiota [53,54]. Because they are

195 the most remarkable groups among the identified substrates, nucleosides,

196 flavonoids, and pollen-specific compounds will be discussed in more detail.

197 *Nucleosides.* Nucleosides are essential biomass components that can also serve

198 as bacterial energy sources. The majority of the honey bee gut microbiota

199 members lack genetic capacity for either purine or pyrimidine biosynthesis [33].

200 Instead, they seem to rely on salvage pathways and the uptake of nucleosides

201   from the environment, providing a likely explanation for the observed depletion

202   of these compounds in the gut of CL bees (**Figure S2A**).

203   *Flavonoids*. Flavonoids are secondary metabolites that can make up 2-4% of the

204   dry weight of pollen [55,56] and this is in concordance with their identification

205   as important diet-derived substrates of the honey bee gut microbiota. Flavonoids

206   typically consist of two phenyl rings and one heterocyclic ring, the so-called

207   aglycone. Glycosylation of this aglycone in diverse positions generates the

208   remarkable flavonoid structural and functional diversity [57]. Among the

209   bacterial substrates we identified several glycosylated flavonoids **(Figure S2B)**

210   that are known to be present in pollen, such as rutin or quercitrin [55]. We

211   unambiguously confirmed the identity of five of these ions as the glycosylated

212   flavonoids afzelin, quercitrin, and rutin using MS/MS fragmentation and spectral

213   similarity calculations (**Supplemental results 1**, **Figure S3, Dataset S3**).

214   Several mammalian gut bacteria can convert flavonoids by either

215   deglycosylation, thus releasing flavonoid aglycones, or C-ring cleavage, resulting

216   in the accumulation of breakdown products of the aromatic backbone [58]. We

217   mined the 132 bacterial products to look for these signatures of flavonoid

218   conversions in the bee gut, and identified several ions annotated as non-

219   glycosylated flavonoids (**Figure S2B**). However, none of them significantly

220   accumulated in CL vs MF bees, which would have been expected when

221   deglycosylation was the only mechanism of flavonoid conversion. Conversely, we

222   identified four ions among the bacterial products that could result from

223   biodegradation of flavonoid aglycones: two ions annotated as hydroxy- and

224   dihydroxyphenylpropionate (*m/z* 165.055, *m/z* 181.050), both of which are

225   known C-ring cleavage products of flavonoids, and two ions annotated as

226   maleylacetate (m/z 157.014) and hydroxy-3-oxoadipate (m/z 175.025), which

227   are intermediates of aromatic compound degradation pathways [59-62] (**Figure**

228   **S2B**). Strikingly, three of these four ions were among the most discriminatory

229   products for CL vs MF bees (**Figure 3**). Moreover, in a recent metabolomics

230   study by Zheng et al (2017) similar aglycone breakdown products were shown

231   to accumulate in the hindgut of colonized bees (**Supplemental results 2,**

232   **Dataset S4**).

233   ***Pollen wall compounds***. The two ions annotated as ω-hydroxy acids (9,10,18-

234   trihydroxystearate, m/z 315.254, and 9,10-dihydroxystearate, m/z 331.249) that

235   were identified among the most discriminatory substrate ions (**Figure 3, Figure**

236   **S2C**) have been reported to be major constituents of sporopollenin [63], the

237   biochemically inert and heterogeneous biopolymer forming the rigid structure of

238   the pollen exine [64]. Phenolamides such as those utilized by the gut microbiota

239   (N1,N5,N10-tricoumaroyl spermidine, m/z 582.260, N1,N5,N10-tricaffeoyl

240   spermidine, m/z 630.245, p-coumaroylputrescine, m/z 233.130, **Figure 3,**

241   **Figure S2C**) are also part of the pollen exine as they are deposited on top and

242   into its cavities as part of the pollen coat [65]. Remarkably, the pollen coat is also

243   where most flavonoids are thought to be located in pollen grains [66].

244   Our findings on the utilization of flavonoids, ω-hydroxy acids and

245   phenolamides thus suggest that the honey bee gut microbiota contributes to the

246   digestion of the rigid outer pollen wall. Easily accessible pollen nutrients (such as

247   amino acids, sugars and vitamins) are likely taken up by the host in the midgut,

248   leaving these more recalcitrant compounds for the microbiota in the hindgut.

249   This is in line with what is know about the biogeography and microbial ecology

250   in the mammalian intestine [67]. Besides being utilized as an energy and carbon

251 source, the conversion of secondary plant metabolites from pollen may have

252 additional benefits for the microbiota and the host. For example, phenolamides

253 and flavonoids both have been reported to exert antimicrobial activities,

254 conceivably because their breakdown products affect the antioxidant potential in

255 the gut which could reduce inflammation and pathogen susceptibility [65,68]. In

256 addition, mammalian flavonoid-metabolizing bacteria have a major impact on

257 the bioavailability of flavonoids, and flavonoids are implicated in modulating

258 weight gain by affecting host signaling [69,70]. This makes it tempting to

259 speculate that flavonoid metabolism in the bee gut contributes to the microbiota-

260 dependent weight gain of honey bees that was observed in a previous study [34].

261

262 **Products of the gut microbiota include fermentation products and host-**

263 **derived metabolites**.

264 We next looked into the 132 ions that were more abundant in CL vs MF bees and

265 thus present possible metabolites produced by the microbiota. Again, we used

266 enrichment analyses and OPLS-DA (**Figure 3**) to prioritize the most important

267 product ions. Three compound classes were to some extent enriched among the

268 bacterial products: *carboxylic acids and derivatives* (7 of 26 detected ions, one-

269 sided Fisher's exact test, P <0.03), *fatty acids and derivatives* (7 of 29 detected

270 ions P <0.05), and *eicosanoids* (5 of 8 detected ions, P <0.01).

271 ***Fermentation products.*** Both the *carboxylic acids and derivatives* and *fatty acids*

272 *and derivatives* categories contain known bacterial fermentation products,

273 several of which accumulated in CL bees (succinate, *m/z* 117.019, pimelate *m/z*

274 159.066, sebacic acid, *m/z* 201.113, butyrate, *m/z* 87.044, valerate *m/z* 101.060).

275 This is in agreement with previous studies showing that fermentation is the

276   dominant metabolism of bee gut bacteria [33,34]. Three of these fermentation

277   products (succinate, pimelate, sebacic acid) were among the 23 most

278   discriminatory products, which highlights the substantial and consistent

279   accumulation of these compounds in the presence of the microbiota (**Figure 3,**

280   **Figure S2D**). Using targeted metabolomics [71] we confirmed the strong

281   accumulation of succinate in the gut of CL bees and determined absolute

282   concentrations of other organic acids in CL and MF bees (**Supplemental results**

283   **3, Figure S4, Dataset S5**). In addition, accumulation of fermentation products is

284   one of the main microbiota-dependent trends found in our study and that of

285   Zheng et al (for details on the comparison see **Supplemental results 2**).

286   *Host-derived metabolites.* The third enriched product category (eicosanoids)

287   includes five ions whose masses match to prostaglandins (**Figure S2E**), which

288   are broadly conserved hormone-like lipids in animals. In insects, prostaglandins

289   have been implicated in reproduction, fluid secretion, and activation of the

290   immune system [72], inducing prophenoloxidase, phagocytosis and hemocyte

291   spreading. None of the five prostaglandins annotated in our study has been

292   functionally characterized in honey bees. Besides eicosanoids, we identified a

293   second group of host-derived metabolites induced by the microbiota. These are

294   three derivatives of juvenile hormone III (**Figure S2E**), two of which were among

295   the most discriminatory product ions (**Figure 3,** *m/z* 283.191 and *m/z* 269.176).

296   Juvenile hormone III plays an important role in regulating growth, development,

297   and reproduction of insects. In adult honey bees, it controls the pace of the

298   developmental maturation from young nurse bees to older forager bees [73].

299   This process is linked to nutrition [74] and could therefore be affected by

300   metabolic activities of gut bacteria. Notably, juvenile hormone derivatives in the

301   gut may have local functions distinct from those in the brain or hemolymph, as

302   was shown for heteropteran linden bugs [75].

303

304   **Gut metabolic profiles of colonized bees and hive bees show substantial**

305   **overlap**.

306   To assess how much of the total metabolic output can be identified in hive bees

307   under natural conditions, we analyzed the gut metabolome of 10-day old hive

308   bees that experienced social interactions, natural dietary sources, and the native

309   gut microbiota. Although principal component analysis revealed that hive bees

310   clustered separately (**Figure S1B**), we found that 27 of the 28 most

311   discriminatory substrate ions and 15 of the 22 most discriminatory product ions

312   showed qualitatively the same changes in hive bees as in CL bees (**Dataset S1,**

313   Welch's t-test, BH adj. P ≤0.01). On the substrate side, this included most

314   flavonoid ions, all nucleosides, quinate, citrate, as well as the ions annotated as

315   ω-hydroxy acids and phenolamides from the outer pollen wall. On the product

316   side, we found four of the five prostaglandins and one of the juvenile hormone

317   derivatives to be significantly increased in hive bees relative to MF bees

318   suggesting that these host-derived metabolites are also induced under natural

319   conditions. Moreover, ions corresponding to fermentation products were either

320   significantly increased (sebacic acid, valerate) or showed a trend towards

321   increased levels (succinate, pimelate) in hive bees. The same was the case for the

322   four ions corresponding to possible degradation products of flavonoids

323   (hydroxy- and dihydroxyphenylpropionate, maleylacetate, hydroxy-3-

324   oxoadipate, **Dataset S1**). Overall, the remarkable overlap of metabolic changes

325   between hive and CL bees highlights the relevance of our findings.

326

Mono-colonizations explain 80% of the overall metabolic output of the honey bee gut microbiota.

We thus far presented evidence for substrates and products of the complete microbiota in the honey bee gut. To elucidate which community members might be responsible for these transformations, we conducted mono-colonizations of MF bees with all seven bacterial species (again using four and two strains together for Firm-5 and *G. apicola,* respectively). All species successfully established in the gut of MF bees without other community members being present (**Figure S5**). We again extracted metabolites from the mid-and hindgut of individual bees to address how many of the 372 robust ion changes can be explained by one or multiple mono-colonizations (**Dataset S1**), i.e. show qualitatively the same change as in CL bees, using analysis of variance (ANOVA followed by Tukey HSD *post hoc* test at 99% confidence, $P \leq 0.05$) (**Dataset S6-S7**).

Remarkably, using these significance cutoffs 299 of the 372 (80%) robust changes between MF and CL bees could be explained by one or multiple mono-colonizations. This included 201 (84%) substrate and 98 (74.%) product ions. The two *Lactobacilli* groups (Firm-5 and Firm-4) explained most changes, followed by *B. asteroides* and the two Gammaproteobacteria (**Figure 4A**). Interestingly, the relative contribution to substrate conversion and product accumulation varied between mono-colonizations. For example, *B. asteroides* contributed relatively little to the conversion of substrates, but seemed to be responsible for the production of a relatively large fraction of bacterial products.

350   The Firm-4 species showed the opposite pattern explaining relatively many

351   bacterial substrates but a small fraction of bacterial products.

352   ***Substrates explained by mono-colonizations.*** We again used enrichment

353   analysis (one-sided Fisher's exact test, $P \leq 0.05$), to get a high-level view of the

354   functions of distinct community members in the conversion or production of

355   certain compound classes (**Figure 4A**). This revealed that all community

356   members, except for *S. alvi* and *B. apis,* contributed to the disappearance of

357   nucleosides in the bee gut (see also **Figure S2A**). Remarkably, *S. alvi* and *B. apis*

358   encode complete nucleoside biosynthesis pathways and therefore do not have to

359   rely on external nucleoside resources. In turn, they seem to preferentially

360   convert carboxylic acids and keto-acids in the gut (malate, *m/z* 133.0139,

361   fumarate, *m/z* 115.003, citrate, *m/z* 191.019, α-ketoglutarate, *m/z* 145.014),

362   which is consistent with the presence of complete TCA cycles and several

363   carboxylate transporters in their genomes [32,54]. Flavonoids were enriched

364   substrates for Firm-5 (11/126 substrate ions, $P<0.01$) and *B. asteroides* (6/55,

365    $P<0.01$), and many flavonoids were also utilized by Firm-4 (7/107, $P=0.051$)

366   (**Figure 4A, Figure S2B**). Interestingly, rutin (*m/z* 609.145) and scolymoside

367   (*m/z* 593.150) were exclusively depleted in the Firm-5 mono-colonization, while

368   afzelin (*m/z* 431.098) was also utilized by Firm-4 and *B. asteroides*, and

369   quercitrin (*m/z* 447.093) even by *G. apicola* (**Figure 4B**). Similar patterns were

370   also found for other flavonoids (**Figure S2B**) suggesting substrate specificity for

371   the utilization of these pollen-derived compounds among community members.

372   In total, 27 of the 28 most discriminatory substrate (**Figure 3**) could be

373   explained by at least one mono-colonization. The two ω-hydroxy acids ions from

374   the outer pollen wall were exclusively utilized by *B. asteroides* and Firm-4 while

375 the three phenolamides from the pollen coat were only depleted in the presence

376 of Firm-5 (**Figure 4C, Figure S2C**). In contrast, quinate and citrate were utilized

377 by several community members suggesting that their almost complete depletion

378 in CL and hive bees could be the result of a communal effort (**Dataset S1**).

379 ***Products explained by monocolonizations.*** For bacterial products, 21 of the 23

380 most discriminatory ions for CL vs MF bees could be explained by at least one

381 mono-colonization. Strikingly, *B. asteroides* explained the accumulation of all

382 host-derived prostaglandins and was also responsible for the induction of two of

383 the three juvenile hormone derivatives, suggesting that this community member

384 has a distinct influence on the host (**Figure 4D, Figure S2E**). Moreover, three

385 major fermentation products that accumulated in CL bees could be explained by

386 mono-colonizations. Succinate (**Figure 3E**) and pimelate ions were produced

387 exclusively in bees colonized with Firm-5 and valerate only in the *B. asteroides*

388 colonized bees (**Figure S2D**, **Dataset S1**). Finally, we found that ions

389 corresponding to putative flavonoid degradation products accumulated in bees

390 colonized with Firm-4 and Firm-5 (**Figure S2B**), which also explained most

391 flavonoid utilization of the bee gut microbiota. This suggests that Firm-4 and

392 Firm-5 do not only deglycosylate flavonoids, via expression of glycoside

393 hydrolases [44], but may additionally degrade the aromatic backbone.

394

395 ***In vitro* recapitulation of metabolic functions of community members**.

396 Our *in vivo* results strongly suggest that specific gut bacteria utilize distinct

397 substrates from the pollen diet of bees. This prompted us to test (i) whether the

398 bacterial species could grow *in vitro* on a pollen-based culture medium and (ii)

399 whether this would result in the metabolic conversions of the same compounds

400   as was observed *in vivo*. To this end, we water-extracted metabolites from the

401   same pollen batch that was used as a dietary source, and analyzed the metabolic

402   composition of this extract using untargeted and targeted metabolomics.

403   Detailed results are presented in the **Supplemental results 4** and show that

404   pollen extracts contain physiologically meaningful levels of nutrients and are

405   expectedly enriched in *amino acids and derivatives*, *flavonoids*, *monosaccharides*,

406   and *carboxylic acids and derivatives* (**Figure S6**). Strikingly, in the presence of

407   this pollen extract, all community members, except for *S. alvi* displayed

408   substantial growth compared to carbon-depleted or reduced control media in

409   which little or no growth was observed after 16 h of incubation (**Figure 5A**).

410   We then profiled the metabolome in growth media before and after

411   bacterial incubation in a separate metabolomics experiment. We annotated a

412   total of 1031 ions (**Dataset S8**) of which 427 (41%) were also present among the

413   1079 ions from the *in vivo* dataset. In line with their growth profiles, the largest

414   number of depleted metabolites (log2(FC) ≥|1| and Welch's t-test BH adj. *P*

415   ≤0.01) were found for the growth cultures of Firm-5, followed by *G. apicola*,

416   Firm-4, *F. perrara*, *B. asteroides*, *B. apis*, and *S. alvi* (**Figure 5A**).

417   Using strict criteria we identified 17 ions - 13 pollen-derived substrates

418   and 4 bacterial products - which were explained *in vivo* and *in vitro* by the same

419   species (**Figure S7, Table S2**). Seven of these 13 substrates belonged to the most

420   discriminatory substrate ions for MF vs CL bees (**Figure 3**): three flavonoids

421   (quercitrin, afzelin, and rutin), one nucleoside (inosine) and ions corresponding

422   to quinate, citrate, and 2-fuorate. The fact that multiple community members

423   were responsible for the conversion of some of these substrates (*B. asteroides*,

424   Firm-4, Firm-5, *F. perrara*, *B. apis* and *G. apicola*) demonstrates that our *in vitro*

425   cultures allowed us to recapitulate metabolic activities covering the whole

426   community.

427   We found remarkably overlapping substrate specificity for four

428   flavonoids *in vitro* and *in vivo* with the Firm-5 species being the only member

429   capable of converting rutin and scolymoside, while quercitrin and afzelin were

430   also utilized by Firm-4, and quercitrin additionally also by *B. asteroides* and *B.*

431   *apis* (**Figure 5A**). Among the four *in vitro* recapitulated products were three of

432   the four ions corresponding to putative breakdown products of flavonoids

433   (**Figure S7, Table S2**). These ions accumulated *in vivo* and *in vitro* in the

434   presence of Firm-4 and/or Firm-5 providing further evidence for breakdown of

435   the polyphenolic ring structure of flavonoids. However, we also found that

436   deglycosylated flavonoids (i.e. aglycones) accumulated in cultures of Firm-4,

437   Firm-5 and *B. asteroides* (**Figure 5A**). Based on this data we suggest that

438   flavonoid degradation involves two steps (**Figure 5B**): (i) deglycosylation of

439   sugar residues and their subsequent fermentation and (ii) the breakdown of the

440   polyphenol backbone. The second step could be relatively slow explaining why

441   aglycones accumulated *in vitro* (16 h), but not *in vivo* (10 days).

442   An obvious difference in our *in vitro* experiments compared to the *in vivo*

443   situation is the presence of the host, which may pre-digest pollen grains before

444   gut bacteria utilize pollen-derived metabolites. For example, certain sugars and

445   amino acids are expected to be present in low amounts *in vivo* because of host

446   absorption. Conversely, the host may also provide metabolites that support

447   growth of some community members. This could explain the poor growth of *S.*

448   *alvi in vitro,* especially since *in vivo S. alvi* is tightly associated with the gut

449   epithelium and other gut bacteria such as *G. apicola* [76].

450

451   **Evidence for cross-feeding in the bee gut microbiota**.

452   Microbial species in gut communities can organize into food chains, where one

453   species provides metabolites that can be utilized by others. Such metabolites

454   may be released from insoluble dietary particles via bacterial degradation or can

455   be generated as waste products of metabolism [2]. To identify possible metabolic

456   interactions between community members of the bee gut microbiota, we focused

457   on ions that *in vivo* significantly accumulated in some mono-colonizations and

458   were depleted in others (**Dataset S1**). A total of 27 ions showed such opposing

459   changes between two or several mono-colonizations (**Table S3**).

460   A striking example of a potential metabolic food chain was the liberation

461   and consumption of one of the major bacterial substrates in CL bees, 9-10-18-

462   trihydroxystearate (*m/z* 331.248), originating from the outer pollen wall. In our

463   mono-colonization experiments, the corresponding ion was depleted in Firm-4

464   and *B. asteroides*, but accumulated in the case of Firm-5 and *G. apicola* (**Figure**

465   **4C**). This suggests that the latter two species facilitate the release of this ω-

466   hydroxy acid from the outer pollen wall making it more accessible for

467   degradation by Firm-4 and *B. asteroides*.

468   A second example is the ion annotated as pyruvate (*m/z* 87.008), which

469   substantially accumulated in the gut of bees mono-colonized with *G. apicola*, but

470   was utilized as a substrate by other bacteria such as *S. alvi* and Firm-5 (**Figure**

471   **6A**). A syntrophic interaction between *G. apicola* and *S. alvi* had previously been

472   suggested, because they are co-localized on the epithelial surface of the ileum

473   [76], and harbor complementary metabolic capabilities [32]. To test for potential

474   cross-feeding of pyruvate from *G. apicola* to *S. alvi*, we supplemented the pollen

475   extract-based medium of *S. alvi* with spent supernatant of *G. apicola* cultures.

476   While growth of *S. alvi* was only weakly improved compared to the control

477   medium (**Figure S8**), metabolome analysis (**Dataset S9**) confirmed that

478   pyruvate and five other ions (**Figure 6B**), which accumulated during the growth

479   of *G. apicola,* were utilized from the conditioned medium by *S. alvi*. The other

480   ions included three fermentation products, a nucleoside derivative, and

481   hydroxyphenylpropionate, which could be a breakdown product of flavonoid

482   degradation by *G. apicola.* These results confirm our predictions from the *in vivo*

483   dataset and show that bee gut bacteria engage in cross-feeding interactions

484   among each other. While not essential for gut colonization in itself as based on

485   our mono-colonization experiments, such interactions are likely important for

486   community resilience and reflect the longstanding coexistence among

487   community members.

488

489   Conclusions

490   The simple composition and experimental amenability of the honey bee gut

491   microbiota facilitated our systems-level approach resulting in the

492   characterization and disentangling of the metabolic potential of a complete gut

493   microbial ecosystem. We reconstituted the honey bee gut microbiota from

494   cultured strains, characterized the metabolic output of the complete microbiota,

495   identified the contributions of individual community members *in vivo*, and

496   recapitulate their activities *in vitro*. Our results provide unprecedented insights

497   into the metabolic functions of bee gut bacteria.

498   As in the mammalian and termite gut ecosystem [1,67], we conclude that

499   most substrates utilized by the bee gut microbiota are indigestible compounds

500   originating from the hosts' diet (**Figure 7**). These include plant metabolites from

501   the outer pollen wall, such as ω-hydroxy acids, phenolamides and flavonoid

502   glycosides. While one of the bee gut bacteria had previously been identified to

503   utilize a major pollen polysaccharide (pectin), our data provides the first

504   evidence for a role of the gut microbiota in breaking down outer pollen wall

505   components. Bacterial fermentation of these pollen-derived compounds resulted

506   in the accumulation of organic acids (e.g. succinate) and polyphenol degradation

507   products, which are likely to impact the physicochemical conditions in the

508   colonized gut. In addition, we found that host-derived signaling molecules are

509   induced by *B. asteroides*, suggesting a specific interaction of this gut symbiont

510   with the host.

511   Based on the mono-colonization experiments, we further conclude that

512   most metabolic output of the bee gut microbiota can be explained by activities of

513   individual community members. These bacteria seem to occupy largely

514   independent yet overlapping metabolic niches in the gut. While we have found

515   evidence for cross-feeding interactions (e.g. between *G. apicola* and *S. alvi*), our

516   findings generally indicate that coevolution of gut bacteria does not necessarily

517   result in interdependencies. This may be generally the case for gut bacteria as

518   they cannot rely on the presence of specific interaction partners in the highly

519   dynamic gut environment, but rather adapt to diet-derived nutrients.

520   The metabolic activities identified in this study are likely key for the

521   symbiotic functions of the bee gut microbiota and thus may be directly linked to

522   its impact on bee health and physiology [34,41]. The fact that we identified many

523   of these metabolic changes in hive bees under natural conditions demonstrates

524   the relevance of our findings and validates the gnotobiotic bee model. Moreover,

525   our study highlights the versatility of high-throughput untargeted metabolomics

526   to disentangle metabolic functions in microbial ecosystems. We believe that this

527   systematic approach can be extended to other gnotobiotic animals to enable a

528   better understanding of the diversity of metabolic activities and functions that

529   are present in microbial communities.

530

Materials and Methods

Honey bee experiments.

MF bees were obtained from a healthy looking colony of *Apis mellifera carnica* located at the University of Lausanne. To this end, dark-eyed pupae were carefully removed from capped brood cells with sterile tweezers and transferred to sterilized plastic boxes as described previously [36]. Boxes with pupae were kept with a source of sterile sugar water (50 % sucrose solution, w/v) at 35°C with 80 – 90 % humidity for the first two days. The temperature was reduced to 32°C on the third day. One or two bees per box were dissected one day prior to colonization and their homogenized hindguts (in 1 ml 1x PBS) were cultured on media as described below to check for sterility of the bee gut. Only healthy looking emerged bees without any deformations and sterile guts were selected for experiments. For colonization of MF bees, bacterial strains were inoculated from glycerol stocks and restreaked twice. Details on bacterial strains and culture conditions can be found in **Table S1**. Bacterial cells were harvested and resuspended in 1x PBS/sugar water (1:1, v/v) at an OD_{600} of 1. For colonization, bacterial suspensions were added to a source of sterilized pollen and provided to the MF bees (for details see **Supplemental methods**). The mid-and hindgut of gnotobiotic bees were dissected at day 10 post colonization and stored at -80°C until further use. To obtain age controlled hive bees, several brood frames without adult bees were transferred from the hive to a ventilated Styrofoam box kept in an incubator at 32 - 34°C in the laboratory overnight. The next day, newly emerged bees were collected, marked on the thorax with a pen and reintroduced into the hive. These bees were recollected 10 days later, and their mid-and hindguts were dissected and stored at -80°C until further use. This experiment

556 was repeated at two different time-points of the year (spring and fall, referred to

557 as experiment 1 and experiment 2 in this study). Whenever possible, we

558 included bees from both experiments in our analysis, such as for CL and MF bees.

559 However, this was not possible for all mono-colonizations due to bacterial

560 contaminations (as detected by qPCR) or in a few cases due to the presence of

561 above-threshold viral loads. The precise numbers of bees included per condition

562 are listed in **Table S4**.

563

564 **Determining bacterial colonization levels in honey bees.**

565 Colonization levels of gut bacteria were determined by qPCR using species-

566 specific primers on DNA samples obtained from the gut tissues also used for

567 metabolomics analysis. Details on DNA/RNA extraction methods are given in

568 **Supplemental methods.** Each DNA sample was screened with eleven different

569 primer pairs targeting the actin gene of *Apis mellifera*, the 16S rRNA gene of all

570 bacteria, and the 16S rRNA gene of nine specific bacterial species (the seven

571 species used this study and two non-core species frequently found in the gut of

572 *Apis mellifera*, Alpha-2.1 and *Lactobacillus kunkeei).* Primers used for this qPCR

573 analysis are summarized in **Table S5**. We also screened all gut samples for the

574 presence of viruses. Samples that were contaminated with other bacteria than

575 the desired ones or which had high virus titers were excluded from the analysis.

576 The MIQE guidelines (minimum information for publication of qPCR

577 experiments) were followed throughout the data analysis of the qPCR

578 experiments [77]. Details on the qPCR analysis can be found in **Supplemental**

579 **methods.**

580

581   ***In vitro* growth on pollen extracts.**

582   Bacteria were pre-cultured on solid media from -80°C glycerol stocks before

583   liquid cultures were inoculated for *in vitro* growth experiments. For *G. apicola*

584   ELS0169, *S. alvi* wkB2, *F. perrara* PEB0191, and *B. apis* PEB0149, we used a

585   modified M9 minimal medium supplemented with casamino acids and vitamins.

586   For *B. asteroides* ELS0168, the Firm-5 strains, and Firm-4 Hon2N^T, we used

587   carbohydrate-free MRS (cfMRS) medium [78]. Bacteria were harvested from

588   plates or spun down from overnight liquid cultures (the latter only for

589   *Lactobacilli* and *B. asteroides*) and resuspended in the corresponding minimal

590   medium. Freshly prepared liquid cultures were supplemented with either 10%

591   (v/v) ddH$_2$O or pollen extract and inoculated at a final OD$_{600}$ of 0.05 (see

592   **Supplemental methods** for details on pollen extract preparation). Half of the

593   culture was immediately processed to determine colony-forming units (CFUs)

594   and to harvest supernatants for metabolomics at time point 0 h, i.e. before

595   growth. The other half of the culture was incubated for 16 h according to the

596   conditions listed in **Table S1** and then processed in the same way. For CFU

597   counting, serial dilutions were plated on solid media and incubated under the

598   species-specific culturing conditions. For metabolomics analysis, the remaining

599   bacterial culture was spun down at 20,000x g at room temperature for 10 min

600   and 300 μl of spent culture supernatant transferred to a fresh tube stored at -

601   80°C until further processing. Five replicates were included for each species and

602   treatment group.

603   For the cross-feeding experiment between *G. apicola* and *S.alvi*, *G.apicola*

604   strain ESL0169 was grown for 8 h in pollen-supplemented M9 medium as

605   described before. Cultures were sterile-filtered and mixed with fresh pollen-

606   supplemented M9 medium 1:1 (v/v). For the control condition, non-inoculated

607   cultures were incubated for 8 h, sterile filtered and mixed with fresh pollen-

608   supplemented M9 medium 1:1 (v/v). Then, *S. alvi* was added to each tube at a

609   final OD_{600} of 0.05. Growth of *S. alvi* was assessed by OD_{600} measurements. For

610   metabolomics analysis, supernatants were sampled at time points 0 h and 8 h for

611   the *G. apicola* conditioning cultures and at time points 0, 16, 36, 72 h for the *S.*

612   *alvi* cultures in conditioned medium.

613

614   **Metabolite extraction and profiling.**

615   Metabolites from gut and pollen samples were water-extracted after mechanical

616   disruption, and supernatants from the *in vitro* experiments were harvested by

617   centrifugation. Detailed methods can be found in the **Supplemental methods**.

618   Gut samples were pre-selected based on their wet-weight (arithmetic mean 55.1

619   mg, standard deviation 9.9). Ten times more water than the gut wet-weight

620   (v/w) was added, and the samples were homogenized with 0.1 mm zirconia

621   beads in a Fast-Prep24™5G homogenizer at 6 m/s for 45 s. This homogenate

622   was snap-frozen in liquid nitrogen for subsequent DNA/RNA extraction, and 20

623   times diluted for metabolite extractions which was achieved by incubating the

624   samples in a pre-heated thermo-mixer at 80°C and 1400 rpm for 3 min. After

625   each minute, the samples were vortexed for 10 s. Subsequently, the samples

626   were centrifuged at 20000x g and 4°C for 5 min, and 150 μl of the resulting

627   supernatant was transferred to a new tube and centrifuged again. Finally, the

628   supernatant was diluted 10x and stored at -80°C or on dry ice for subsequent

629   metabolomics analysis.

630   Samples were injected into an Agilent 6550 time-of-flight mass

631   spectrometer (ESI-iFunnel Q-TOF, Agilent Technologies) operated in negative

632   mode, at 4 Ghz, high resolution, and with a mass / charge (m/z) range of 50-1000

633   [21]. The mobile phase was 60:40 isopropanol:water (v/v) and 1 mM NH_4F at pH

634   9.0 supplemented with hexakis (1H, 1H, 3H- tetrafluoropropoxy)phosphazine

635   and 3-amino-1-propanesulfonic acid for online mass correction. After processing

636   of raw data as described in [21], m/z features (ions) were annotated by matching

637   their accurate mass to sum formulas of compounds in the Kyoto Encyclopedia of

638   Genes and Genomes (KEGG) database with 0.001 Da mass accuracy and

639   accounting for deprotonation $[M-H^+]^-$. This method cannot distinguish between

640   isobaric compounds, e.g. metabolites having identical m/z values. The raw data

641   of samples from the three sets of experiments (bee gut samples, *in vitro*

642   supernatants, and cross-feeding supernatants) were processed and annotated

643   separately to accommodate their different sample matrices or times of

644   measurement. This data can be explored in **Dataset S1**, **S8, and S9**. Raw data

645   processing and annotation took place in Matlab (The Mathworks, Natick) as

646   described previously [21] and downstream processing and statistical tests were

647   performed in R (R Foundation for Statistical Computing, Vienna, Austria).

648   Selected metabolite samples were measured in targeted fashion using

649   ultra-high-pressure chromatography-coupled tandem mass spectrometry as

650   described before [71]. Metabolite quantifications were performed by

651   interpolating observed intensities to a standard curve of the metabolite.

652   Flavonoid ions were targeted for MS/MS fragmentation as $[M-H^+]^-$

653   electrospray derivatives with a window size of ± 4 m/z in Q1. Fragmentation of

654   the precursor ion was performed by collision-induced dissociation at 0, 10, 20,

655   and 40 eV collision energy and fragment-ion spectra were recorded in scanning

656   mode by high-resolution time-of-flight MS. Spectra were interpreted using

657   MetFrag (Ruttkies *et al.*, 2016), and spectral cosine similarity scores were

658   calculated between reference spectra that were obtained in-house or library

659   spectra   from   MassBank   of   North   America   (MoNA,

660   http://mona.fiehnlab.ucdavis.edu/). For further details see **Supplemental**

661   **methods.**

662

663   **Untargeted metabolomics data analysis.**

664   All steps of the downstream data analysis were performed in R (R Foundation for

665   Statistical Computing, Vienna, Austria). Samples from double injections

666   (technical replicates) were confirmed to be highly similar and averaged.

667   Subsequent analyses were performed on these averaged ion intensities, which

668   are available in **Dataset S1**, **Dataset S8**, and **Dataset 9**.

669   Ions that were deemed robustly different between the MF and CL bees

670   were those that were significantly different (Welch t-test, BH adj. *P* ≤0.01)

671   between CL and MF in both independent experiments. Differences between MF

672   and CL samples were expressed as log2(fold-change) values for both

673   experiments separately and for pooled data of both experiments (see **Dataset**

674   **S1**).

675   Enrichment analyses were computed on compound class categories from

676   KEGG (in house database), which are added in the column "compound class" in

677   **Dataset S1**. Some ions with ambiguous annotations had a compound class

678   associated to multiple of these annotations. However, supported by the

679   observation that compound classes between alternative annotations were often

680 the same (or highly related) only the compound class of the first annotation was

681 used as input for one-sided Fischer's exact tests (**Dataset S3**).

682 One-way analysis of variance (ANOVA) was performed between all bee

683 gut samples after selecting the relevant samples from the data matrix and

684 normalizing the intensities to ion standard (Z-) scores (i.e. by row). The results

685 of the full ANOVA analysis can be explored in **Dataset S6**. For this study the

686 focus was on differences between any group and MF bees which were

687 considered significant when having an Tukey HSD *post hoc* adjusted *P*-value ≤

688 0.05. When for a specific monocolonization group this significance cut-off was

689 met and the direction of the change was the same as that for CL vs MF, the ion

690 was considered to be "explained" by this group.

691 In order to enrich for pollen ions we only considered ions with an

692 arithmetic mean intensity of ≥10,000 in the pollen samples, in addition to being

693 highly significantly different from water-matrix control samples (Welch t-test,

694 BH adj. ≤ 0.001) and displaying a large (≥ 2) log2(fold change) difference.

695 For the *in vitro* data (**Dataset S8**), the goal was to identify pollen

696 substrates and bacterial products for which changes in levels were observed *in*

697 *vivo* and *in vitro*. Pollen ions were mapped by matching the top annotation

698 formula of both datasets. For all media-strain combinations we performed a

699 statistical comparison between time point 16 h and 0 h and considered only

700 those ions with a log2(fold change) of ≥|1| and BH adj. *P*-value of ≤0.01 as

701 significant *in vitro* products or substrates. In order to be certain that only pollen-

702 derived substrates were included, for every strain only ions that displayed a

703 significant negative log2(fold change) exclusively in the base medium

704 supplemented with pollen extract were considered as *in vitro* pollen substrates.

Main text

705   To identify ions that might be cross-fed between *G. apicola* and *S. alvi*,

706   ions were selected that increased during the growth of *G. apicola* and were

707   depleted when *S. alvi* was grown in this conditioned medium mixed 1:1 with

708   fresh base medium. To do this all ion intensities for both strains (**Dataset S9**)

709   were split and transformed to log2(fold-change) with respect to the first time

710   point of sampling. Ions that had a total log2(fold change) of ≥|1| during *G. apicola*

711   growth and a total log2(fold change) of ≤|-1| during *S. alvi* growth were selected.

712   For a more extensive version of these methods including settings of

713   functions, and detailed protocols see **Supplemental methods.**

714

715

716 **Author Contributions**

717 Conceptualization, L.K., R.A.T.M., K.E., U.S., and P.E.; Methodology, L.K., R.A.T.M.,

718 and P.E.; Validation, L.K., R.A.T.M., and P.E.; Investigation, L.K., R.A.T.M., and P.E.;

719 Supervision, U.S. and P.E.; Writing – Original Draft, L.K., R.A.T.M., and P.E.;

720 Funding Acquisition, U.S. and P.E.

721

Acknowledgements

References

1. Brune A. Symbiotic digestion of lignocellulose in termite guts. Nat Rev Microbiol. 2014;12: 168–180. doi:10.1038/nrmicro3182

2. Koropatkin NM, Cameron EA, Martens EC. How glycan metabolism shapes the human gut microbiota. Nat Rev Microbiol. 2012;10: 323–335. doi:10.1038/nrmicro2746

3. Engel P, Moran NA. The gut microbiota of insects - diversity in structure and function. FEMS Microbiol Rev. 2013;37: 699–735. doi:10.1111/1574-6976.12025

4. Shin SC, Kim S-H, You H, Kim B, Kim AC, Lee K-A, et al. *Drosophila* microbiome modulates host developmental and metabolic homeostasis via insulin signaling. Science. 2011;334: 670–674. doi:10.1126/science.1212782

5. Storelli G, Defaye A, Erkosar B, Hols P, Royet J, Leulier F. *Lactobacillus plantarum* promotes *Drosophila* systemic growth by modulating hormonal signals through TOR-dependent nutrient sensing. Cell Metab. 2011;14: 403–414. doi:10.1016/j.cmet.2011.07.012

6. Blanton LV, Charbonneau MR, Salih T, Barratt MJ, Venkatesh S, Ilkaveya O, et al. Gut bacteria that prevent growth impairments transmitted by microbiota from malnourished children. Science. 2016;351: aad3311–aad3311. doi:10.1126/science.aad3311

7. Schwarzer M, Makki K, Storelli G, Machuca-Gayet I, Srutkova D, Hermanova P, et al. *Lactobacillus plantarum* strain maintains growth of infant mice during chronic undernutrition. Science. 2016;351: 854–857. doi:10.1126/science.aad8588

8. Smith PM, Howitt MR, Panikov N, Michaud M, Gallini CA, Bohlooly-Y M, et al. The microbial metabolites, short-chain fatty acids, regulate colonic Treg cell homeostasis. Science. 2013;341: 569–573. doi:10.1126/science.1241165

9. Trompette A, Gollwitzer ES, Yadava K, Sichelstiel AK, Sprenger N, Ngom-Bru C, et al. Gut microbiota metabolism of dietary fiber influences allergic airway disease and hematopoiesis. Nat Med. 2014;20: 159–166. doi:10.1038/nm.3444

10. Rooks MG, Garrett WS. Gut microbiota, metabolites and host immunity. Nat Rev Immunol. 2016;16: 341–352. doi:10.1038/nri.2016.42

11. Stecher B, Hardt W-D. Mechanisms controlling pathogen colonization of the gut. Curr Opin Microbiol. 2011;14: 82–91. doi:10.1016/j.mib.2010.10.003

768   12.   Blaut M, Clavel T. Metabolic diversity of the intestinal microbiota:
769   implications for health and disease. J Nutr. 2007;137: 751S–5S.

770   13.   Ley RE, Hamady M, Lozupone C, Turnbaugh PJ, Ramey RR, Bircher JS, et al.
771   Evolution of mammals and their gut microbes. Science. 2008;320: 1647–
772   1651. doi:10.1126/science.1155725

773   14.   Conlon MA, Bird AR. The impact of diet and lifestyle on gut microbiota and
774   human health. Nutrients. 2014;7: 17–44. doi:10.3390/nu7010017

775   15.   Engel P, Martinson VG, Moran NA. Functional diversity within the simple
776   gut microbiota of the honey bee. Proc Natl Acad Sci USA. 2012;109:
777   11002–11007. doi:10.1073/pnas.1202970109

778   16.   Warnecke F, Luginbühl P, Ivanova N, Ghassemian M, Richardson TH, Stege
779   JT, et al. Metagenomic and functional analysis of hindgut microbiota of a
780   wood-feeding higher termite. Nature. 2007;450: 560–565.
781   doi:10.1038/nature06269

782   17.   Hess M, Sczyrba A, Egan R, Kim T-W, Chokhawala H, Schroth G, et al.
783   Metagenomic Discovery of Biomass-Degrading Genes and Genomes from
784   Cow Rumen. Science. 2011;331: 463–467. doi:10.1126/science.1200387

785   18.   Qin J, Li R, Raes J, Arumugam M, Burgdorf KS, Manichanh C, et al. A human
786   gut microbial gene catalogue established by metagenomic sequencing.
787   Nature. 2010;464: 59–65. doi:10.1038/nature08821

788   19.   Patti GJ, Yanes O, Siuzdak G. Innovation: Metabolomics: the apogee of the
789   omics trilogy. Nat Rev Mol Cell Biol. 2012;13: 263–269.
790   doi:10.1038/nrm3314

791   20.   Sévin DC, Kuehne A, Zamboni N, Sauer U. Biological insights through
792   nontargeted metabolomics. Curr Opin Biotechnol. 2015;34: 1–8.
793   doi:10.1016/j.copbio.2014.10.001

794   21.   Fuhrer T, Heer D, Begemann B, Zamboni N. High-throughput, accurate
795   mass metabolome profiling of cellular extracts by flow injection-time-of-
796   flight mass spectrometry. Anal Chem. 2011;83: 7074–7080.
797   doi:10.1021/ac201267k

798   22.   Martin F-PJ, Sprenger N, Montoliu I, Rezzi S, Kochhar S, Nicholson JK.
799   Dietary modulation of gut functional ecology studied by fecal
800   metabonomics. J Proteome Res. 2010;9: 5284–5295.
801   doi:10.1021/pr100554m

802   23.   Holmes E, Li JV, Marchesi JR, Nicholson JK. Gut microbiota composition and
803   activity in relation to host metabolic phenotype and disease risk. Cell
804   Metab. 2012;16: 559–564. doi:10.1016/j.cmet.2012.10.007

805   24.   Daniel H, Gholami AM, Berry D, Desmarchelier C, Hahne H, Loh G, et al.
806   High-fat diet alters gut microbiota physiology in mice. ISME J. 2014;8:

807   295–308. doi:10.1038/ismej.2013.155

808   25. Walker A, Pfitzner B, Neschen S, Kahle M, Harir M, Lucio M, et al. Distinct
809   signatures of host-microbial meta-metabolome and gut microbiome in two
810   C57BL/6 strains under high-fat diet. ISME J. 2014;8: 2380–2396.
811   doi:10.1038/ismej.2014.79

812   26. Ridaura VK, Faith JJ, Rey FE, Cheng J, Duncan AE, Kau AL, et al. Gut
813   microbiota from twins discordant for obesity modulate metabolism in
814   mice. Science; 2013;341: 1241214–1241214.
815   doi:10.1126/science.1241214

816   27. Lu K, Abo RP, Schlieper KA, Graffam ME, Levine S, Wishnok JS, et al.
817   Arsenic exposure perturbs the gut microbiome and its metabolic profile in
818   mice: an integrated metagenomics and metabolomics analysis. Environ
819   Health Perspect. 2014;122: 284–291. doi:10.1289/ehp.1307429

820   28. Weir TL, Manter DK, Sheflin AM, Barnett BA, Heuberger AL, Ryan EP. Stool
821   microbiome and metabolome differences between colorectal cancer
822   patients and healthy adults. PLoS ONE; 2013;8: e70803.
823   doi:10.1371/journal.pone.0070803

824   29. Theriot CM, Koenigsknecht MJ, Carlson PE, Hatton GE, Nelson AM, Li B, et
825   al. Antibiotic-induced shifts in the mouse gut microbiome and metabolome
826   increase susceptibility to *Clostridium difficile* infection. Nat Commun.
827   Nature Publishing Group; 2014;5: 3114. doi:10.1038/ncomms4114

828   30. Wang Z, Klipfell E, Bennett BJ, Koeth R, Levison BS, Dugar B, et al. Gut flora
829   metabolism of phosphatidylcholine promotes cardiovascular disease.
830   Nature. 2011;472: 57–63. doi:10.1038/nature09922

831   31. Kwong WK, Medina LA, Koch H, Sing K-W, Soh EJY, Ascher JS, et al.
832   Dynamic microbiome evolution in social bees. Science Advances. 2017;3:
833   e1600513. doi:10.1126/sciadv.1600513

834   32. Kwong WK, Engel P, Koch H, Moran NA. Genomics and host specialization
835   of honey bee and bumble bee gut symbionts. Proc Natl Acad Sci USA.
836   National Acad Sciences. 2014;111: 11509–11514.
837   doi:10.1073/pnas.1405838111

838   33. Kwong WK, Moran NA. Gut microbial communities of social bees. Nat Rev
839   Microbiol. 2016;14: 374–384. doi:10.1038/nrmicro.2016.43

840   34. Zheng H, Powell JE, Steele MI, Dietrich C, Moran NA. Honeybee gut
841   microbiota promotes host weight gain via bacterial metabolism and
842   hormonal signaling. Proc Natl Acad Sci USA. 2017;54: 201701819.
843   doi:10.1073/pnas.1701819114

844   35. Kwong WK, Mancenido AL, Moran NA. Immune system stimulation by the
845   native gut microbiota of honey bees. R Soc Open Sci. 2017;4: 170003.
846   doi:10.1098/rsos.170003

847   36.   Emery O, Schmidt K, Engel P. Immune system stimulation by the gut
848   symbiont *Frischella perrara* in the honey bee (*Apis mellifera*). Molecular
849   Ecology. 2017;50: 735. doi:10.1111/mec.14058

850   37.   Gallai N, Salles J-M, Settele J, Vaissière BE. Economic valuation of the
851   vulnerability of world agriculture confronted with pollinator decline.
852   Ecological Economics. 2009;68: 810–821.
853   doi:10.1016/j.ecolecon.2008.06.014

854   38.   Potts SG, Biesmeijer JC, Kremen C, Neumann P, Schweiger O, Kunin WE.
855   Global pollinator declines: trends, impacts and drivers. Trends in Ecology
856   & Evolution. 2010;25: 345–353.

857   39.   Engel P, Kwong WK, McFrederick Q, Anderson KE, Barribeau SM, Chandler
858   JA, et al. The Bee Microbiome: Impact on Bee Health and Model for
859   Evolution and Ecology of Host-Microbe Interactions. MBio. 2016;7:
860   e02164–15. doi:10.1128/mBio.02164-15

861   40.   Schwarz RS, Moran NA, Evans JD. Early gut colonizers shape parasite
862   susceptibility and microbiota composition in honey bee workers. Proc Natl
863   Acad Sci USA. 2016;: 201606631. doi:10.1073/pnas.1606631113

864   41.   Raymann K, Shaffer Z, Moran NA. Antibiotic exposure perturbs the gut
865   microbiota and elevates mortality in honeybees. Gore J, editor. PLoS Biol.
866   2017;15: e2001861. doi:10.1371/journal.pbio.2001861

867   42.   Cox-Foster DL, Conlan S, Holmes EC, Palacios G, Evans JD, Moran NA, et al.
868   A metagenomic survey of microbes in honey bee colony collapse disorder.
869   Science. 2007;318: 283–287. doi:10.1126/science.1146498

870   43.   Engel P, Vizcaino MI, Crawford JM. Gut Symbionts from Distinct Hosts
871   Exhibit Genotoxic Activity via Divergent Colibactin Biosynthesis Pathways.
872   Appl Environ Microbiol. 2015;81: 1502–1512. doi:10.1128/AEM.03283-14

873   44.   Ellegaard KM, Tamarit D, Javelind E, Olofsson TC, Andersson SGE, Vásquez
874   A. Extensive intra-phylotype diversity in lactobacilli and bifidobacteria
875   from the honeybee gut. BMC Genomics. 2015;16: 284.
876   doi:10.1186/s12864-015-1476-6

877   45.   Roulston TH, Cane JH. Pollen nutritional content and digestibility for
878   animals. Pollen and Pollination. Plant System Evol. 2000;222:187–209.
879   doi:10.1007/978-3-7091-6306-1_10

880   46.   Crailsheim K. The protein balance of the honey bee worker. Apidologie.
881   1990;21:417-429. doi:10.1051/apido:19900504

882   47.   Crailsheim K. Intestinal transport of sugars in the honeybee (*Apis mellifera*
883   L.). J Insect Physiol. 1988;34: 839–845. doi:10.1016/0022-
884   1910(88)90117-5

885   48.   Engel P, Stepanauskas R, Moran NA. Hidden diversity in honey bee gut

886   symbionts detected by single-cell genomics. PLoS Genet. 2014;10:
887   e1004596. doi:10.1371/journal.pgen.1004596

888 49. Powell JE, Martinson VG, Urban-Mead K, Moran NA. Routes of acquisition
889   of the gut microbiota of the honey bee *Apis mellifer*a. Appl Environ
890   Microbiol. 2014;80: 7378–7387. doi:10.1128/AEM.01861-14

891 50. Moran NA, Hansen AK, Powell JE, Sabree ZL. Distinctive gut microbiota of
892   honey bees assessed using deep sampling from individual worker bees.
893   PLoS ONE. 2012;7: e36393. doi:10.1371/journal.pone.0036393

894 51. Corby-Harris V, Maes P, Anderson KE. The bacterial communities
895   associated with honey bee (*Apis mellifera*) foragers. PLoS ONE. 2014;9:
896   e95056. doi:10.1371/journal.pone.0095056

897 52. Brereton RG, Lloyd GR. Partial least squares discriminant analysis: taking
898   the magic away. J Chemometr. 2014;28: 213–225. doi:10.1002/cem.2609

899 53. Kwong WK, Moran NA. Cultivation and characterization of the gut
900   symbionts of honey bees and bumble bees: description of *Snodgrassella*
901   *alvi* gen. nov., sp. nov., a member of the family *Neisseriaceae* of the
902   *Betaproteobacteria*, and *Gilliamella apicola* gen. nov., sp. nov., a member of
903   *Orbaceae* fam. nov., *Orbales* ord. nov., a sister taxon to the order
904   "*Enterobacteriales*" of the *Gammaproteobacteria*. Int J Syst Evol Microbiol.
905   2013;63: 2008–2018. doi:10.1099/ijs.0.044875-0

906 54. Segers FH, Kešnerová L, Kosoy M, Engel P. Genomic changes associated
907   with the evolutionary transition of an insect gut symbiont into a blood-
908   borne pathogen. ISME J. 2017;60: 810. doi:10.1038/ismej.2016.201

909 55. Rzepecka-Stojko A, Stojko J, Kurek-Górecka A, Górecki M, Kabała-Dzik A,
910   Kubina R, et al. Polyphenols from Bee Pollen: Structure, Absorption,
911   Metabolism and Biological Activity. Molecules. 2015;20: 21732–21749.
912   doi:10.3390/molecules201219800

913 56. Falcone Ferreyra ML, Rius SP, Casati P. Flavonoids: biosynthesis, biological
914   functions, and biotechnological applications. Front Plant Science. 2012;3:
915   222. doi:10.3389/fpls.2012.00222

916 57. Le Roy J, Huss B, Creach A, Hawkins S, Neutelings G. Glycosylation Is a
917   Major Regulator of Phenylpropanoid Availability and Biological Activity in
918   Plants. Front Plant Science. 2016;7: 735. doi:10.3389/fpls.2016.00735

919 58. Braune A, Blaut M. Bacterial species involved in the conversion of dietary
920   flavonoids in the human gut. Gut Microbes. 2016;7: 216–234.
921   doi:10.1080/19490976.2016.1158395

922 59. Labib S, Erb A, Kraus M, Wickert T, Richling E. The pig caecum model: A
923   suitable tool to study the intestinal metabolism of flavonoids. Mol Nutr
924   Food Res. 2004;48: 326–332. doi:10.1002/mnfr.200400022

925   60.   Schoefer L, Mohan R, Schwiertz A, Braune A, Blaut M. Anaerobic
926   degradation of flavonoids by *Clostridium orbiscindens*. Appl Environ
927   Microbiol. 2003;69: 5849–5854. doi:10.1128/AEM.69.10.5849-5854.2003

928   61.   Simmering R, Pforte H, Jacobasch G, Blaut M. The growth of the flavonoid-
929   degrading intestinal bacterium, *Eubacterium ramulus,* is stimulated by
930   dietary flavonoids in vivo. FEMS Microbiology Ecology. 2002;40: 243–248.
931   doi:10.1111/j.1574-6941.2002.tb00957.x

932   62.   Hopper W, Mahadevan A. Degradation of catechin by *Bradyrhizobium*
933   *japonicum*. Biodegradation. 1997;8: 159–165.
934   doi:10.1023/A:1008254812074

935   63.   Li H, Zhang D. Biosynthesis of anther cuticle and pollen exine in rice. Plant
936   Signal Behav. 2010;5: 1121–1123. doi:10.4161/psb.5.9.12562

937   64.   Ariizumi T, Toriyama K. Genetic regulation of sporopollenin synthesis and
938   pollen exine development. Annu Rev Plant Biol. 2011;62: 437–460.
939   doi:10.1146/annurev-arplant-042809-112312

940   65.   Bassard J-E, Ullmann P, Bernier F, Werck-Reichhart D. Phenolamides:
941   Bridging polyamines to the phenolic metabolism. Phytochemistry.
942   2010;71: 1808–1824.

943   66.   Wiermann R, Vieth K. Outer pollen wall, an important accumulation site
944   for flavonoids. Protoplasma. 1983;118: 230–233.
945   doi:10.1007/BF01281807

946   67.   Donaldson GP, Lee SM, Mazmanian SK. Gut biogeography of the bacterial
947   microbiota. Nat Rev Microbiol. 2016;14: 20–32. doi:10.1038/nrmicro3552

948   68.   Cushnie TPT, Lamb AJ. Antimicrobial activity of flavonoids. Int J
949   Antimicrob Agents. 2005;26: 343–356.

950   69.   Kaakoush NO, Morris MJ. More Flavor for Flavonoid-Based Interventions?
951   Trends Mol Med. 2017. doi:10.1016/j.molmed.2017.02.008

952   70.   Thaiss CA, Itav S, Rothschild D, Meijer M, Levy M, Moresi C, et al. Persistent
953   microbiome alterations modulate the rate of post-dieting weight regain.
954   Nature. 2016;540: 544–551. doi:10.1038/nature20796

955   71.   Buescher JM, Moco S, Sauer U, Zamboni N. Ultrahigh Performance Liquid
956   Chromatography–Tandem Mass Spectrometry Method for Fast and Robust
957   Quantification of Anionic and Aromatic Metabolites. Anal Chem. 2010;82:
958   4403–4412. doi:10.1021/ac100101d

959   72.   Stanley D, Kim Y. Prostaglandins and their receptors in insect biology.
960   Front Endocrinol. 2011;2: 105. doi:10.3389/fendo.2011.00105

961   73.   Robinson GE, Page RE, Strambi C, Strambi A. Hormonal and genetic control
962   of behavioral integration in honey bee colonies. Science. 1989;246: 109–

963   112. doi:10.1126/science.246.4926.109

964   74.   Toth AL, Kantarovich S, Meisel AF, Robinson GE. Nutritional status
965   influences socially regulated foraging ontogeny in honey bees. Journal of
966   Experimental Biology. 2005;208: 4641–4649. doi:10.1242/jeb.01956

967   75.   Noriega FG. Juvenile Hormone Biosynthesis in Insects: What Is New, What
968   Do We Know, and What Questions Remain? International Scholarly
969   Research Notices. Hindawi Publishing Corporation; 2014;2014: 1–16.
970   doi:10.1155/2014/967361

971   76.   Martinson VG, Moy J, Moran NA. Establishment of characteristic gut
972   bacteria during development of the honeybee worker. Appl Environ
973   Microbiol. 2012;78: 2830–2840. doi:10.1128/AEM.07810-11

974   77.   Bustin SA, Benes V, Garson JA, Hellemans J, Huggett J, Kubista M, et al. The
975   MIQE Guidelines: Minimum Information for Publication of Quantitative
976   Real-Time PCR Experiments. Clin Chem. 2009;55: 611–622.
977   doi:10.1373/clinchem.2008.112797

978   78.   O'Donnell MM, Forde BM, Neville B, Ross PR, O'Toole PW. Carbohydrate
979   catabolic flexibility in the mammalian intestinal commensal Lactobacillus
980   ruminis revealed by fermentation studies aligned to genome annotations.
981   Microb Cell Fact. 2011;10 Suppl 1: S12. doi:10.1186/1475-2859-10-S1-
982   S12

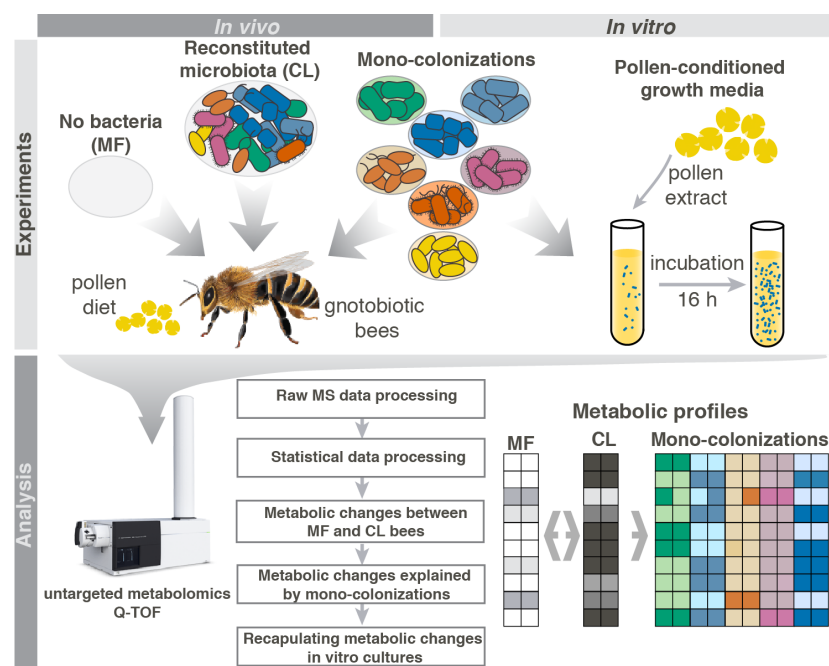983
984

985 **Figures**
986

987

988 **Figure 1. Overview of the experimental setup to characterize metabolic**

989 **activities of the honey bee gut microbiota**. Newly emerged adult bees were

990 either kept microbiota-free, colonized with a reconstituted community of the

991 seven predominant species of the bee gut microbiota (CL), or monocolonized

992 with one of the seven species separately. Bees obtained gamma-sterilized bee

993 pollen as diet. Ten days after colonization honey bee guts were extracted and

994 subjected to untargeted metabolomics to (i) reveal overall metabolomics

995 changes in CL vs MF bees and (ii) to identify which community member could

996 explain these metabolic changes in the gut. As a control, we additionally analyzed

997 10-day old hive bees that were colonized by the native microbiota under natural

998 conditions in the colony (not shown in this figure). To recapitulate findings *in*

999 *vitro*, individual community members were cultured in pollen-conditioned

1000 medium and metabolic changes in this medium were again profiled using

1001 untargeted metabolomics.

1002

1003
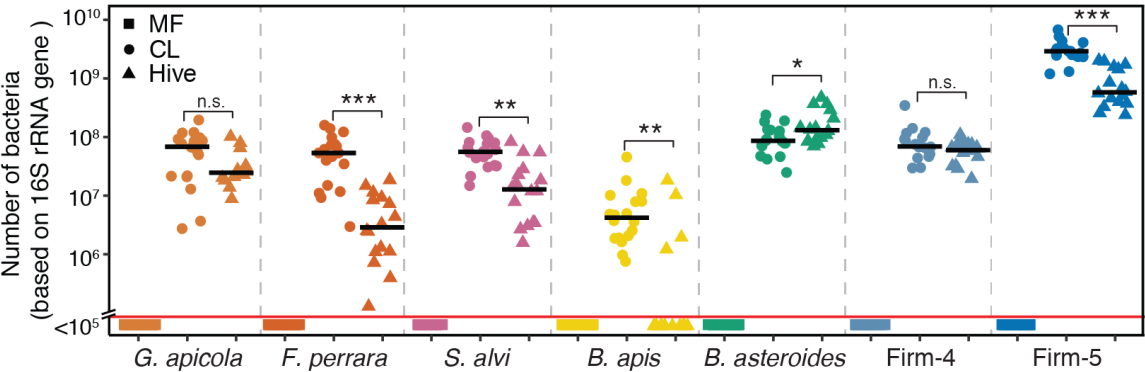
1004 **Figure 2. Colonization levels of the seven community members in guts of**

1005 **microbiota-free bees (MF), colonized bees (CL), and hive bees.** (A) Bacterial

1006 loads in the mid/hindguts of 10-day old MF bees (n= 21), CL bees (n= 18), and

1007 hive bees (n = 16) were assessed by quantitative PCR of the 16S rRNA gene using

1008 species-specific primer pairs. Black lines show median values. Samples shown

1009 below the red line had $<10^5$ bacterial cells per gut. Primer characteristics are

1010 summarized in **Table S5**.

1011
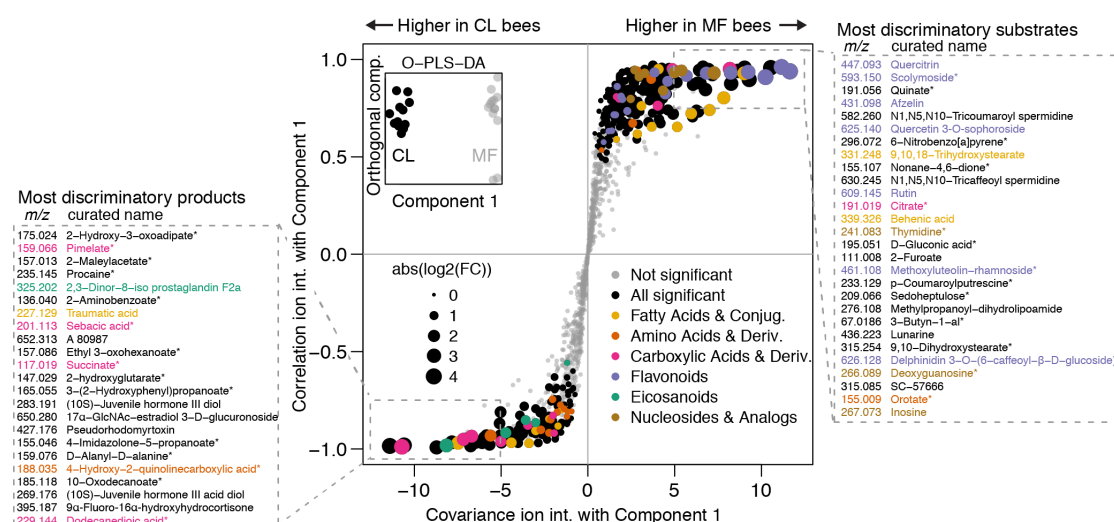
Figure 3. Metabolite changes between microbiota-free (MF) bees and bees colonized with the reconstituted microbiota (CL). Orthogonal Projection of Least Squares-Differentiation Analysis (OPLS-DA) based S-plot of metabolite changes shows ions responsible for MF and CL separation. Inset shows OPLS-DA separation between MF and CL along the component that was used for correlating ion intensities. Experiment 2 data (see **Dataset 1**) was used for this plot, and annotated ions that were not robustly significantly different between MF and CL in both experiments are plotted in grey. Ions with a first annotation belonging to an enriched category are plotted in color (see **Dataset 2**), except for the category *amino acids and derivatives* which did not meet the significance threshold for enrichment but was deemed relevant. The *purine-* and *pyrimidine nucleosides and analogues* categories were combined into *nucleosides and analogs* for coloring only. The boxed areas show the *m/z* [M-H$^+$]$^-$ of the ion and the first annotation name of the most discriminatory ions, sorted by covariance. Asterisks indicate ions with ambiguous annotations.
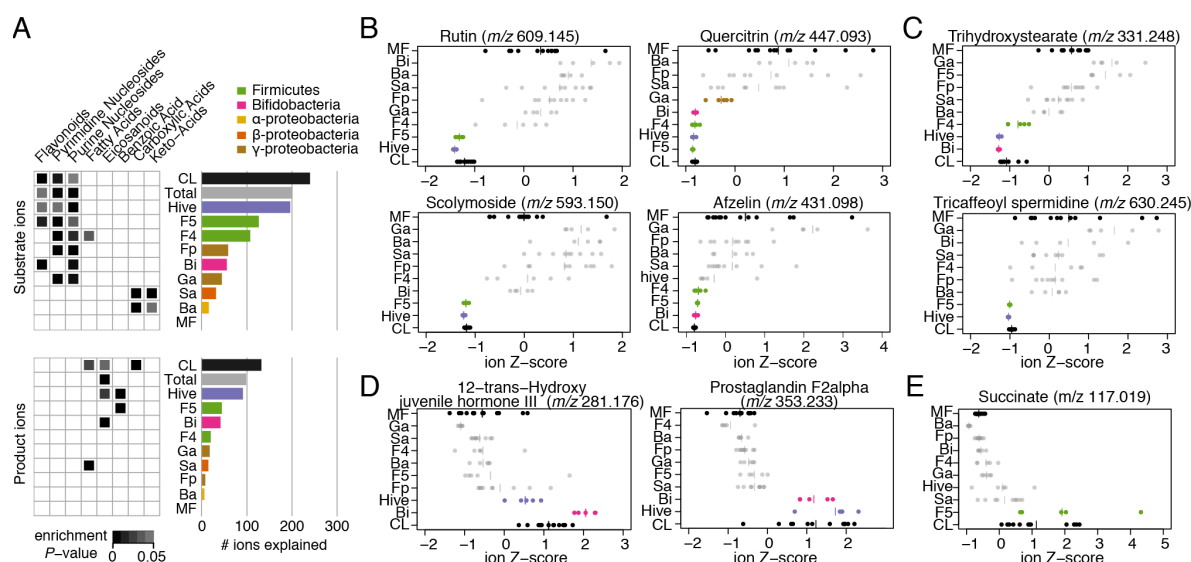
Figure 4. Overview of metabolite changes explained by different community members of the bee gut microbiota. (A) Distribution of metabolic changes explained by mono-colonizations. Bar graphs show distribution of the substrates (240 ions) and products (132 ions) separately. Enrichment P-values (one-sided Fisher's exact test) are provided for compound categories enriched in one or several mono-colonizations. The results of the full enrichment analysis are provided in **Dataset S2**. (B-E) Z-score transformed ion intensity of selected substrate and product ions are shown for all treatment groups. (B) glycosylated flavonoid substrates, (C) two substrates from the outer pollen wall, (D) two products corresponding to host-derived metabolites, (E) succinate, one of the major fermentation products. Groups depicted in color highlight treatment groups displaying a significant difference compared to MF bees in the same direction as the MF vs CL difference (one-way ANOVA, Tukey HSD *post hoc* test at 99% confidence, $P \leq 0.05$). Plots for all 372 ions are provided in **Dataset S7**. MF, microbiota-free, Ba, *Bartonella apis* mono-colonized, Bi, *Bifidobacterium asteroides* mono-colonized, F4, Firm-4 mono-colonized, F5, Firm-5 mono-colonized, Fp, *Frischella perrara* mono-colonized, Ga, *Gilliamella apicola* mono-

1046   colonized, Sa, *Snodgrassella alvi* mono-colonized, CL, colonized with the

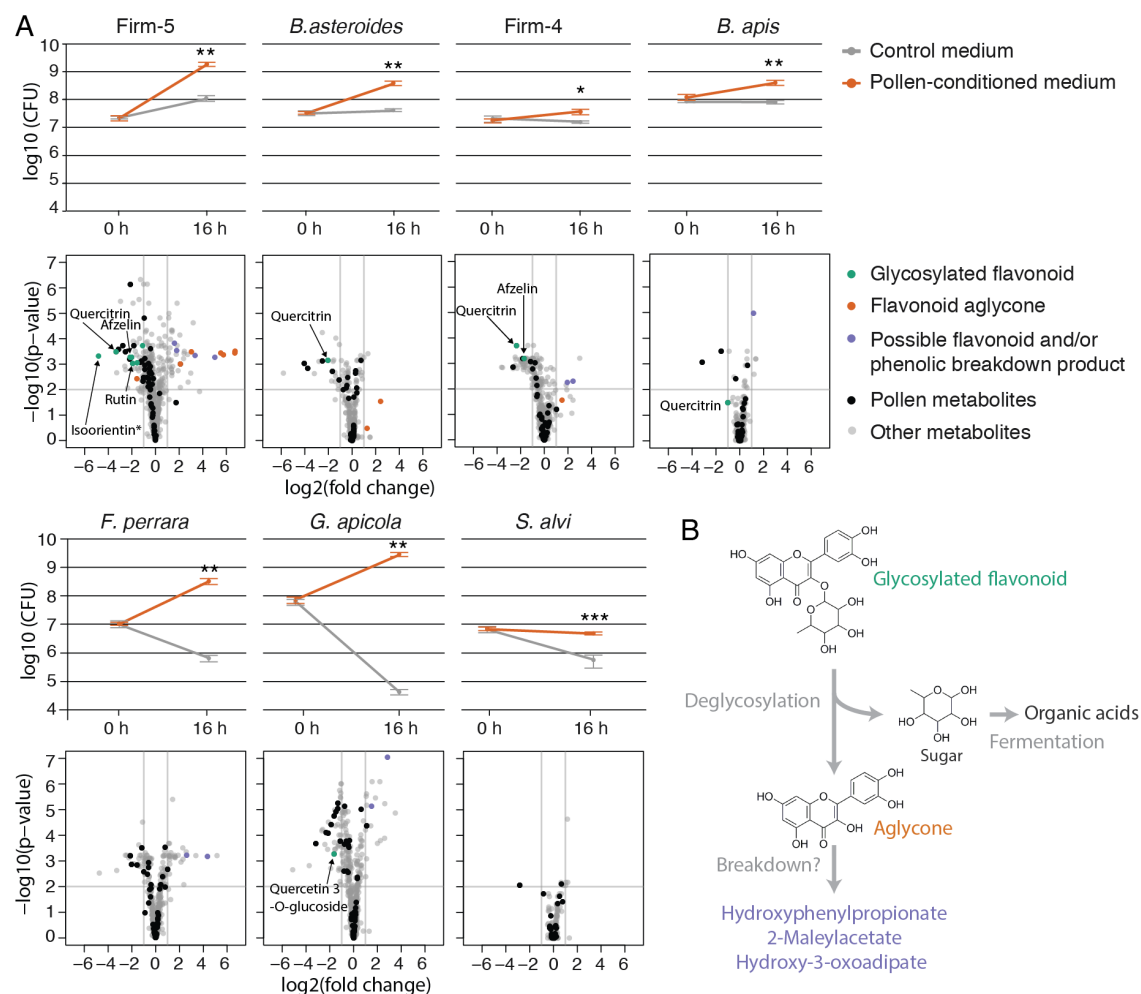1047   reconstituted microbiota, hive, hive bees.

1048

Figure 5. Recapitulation of metabolic changes induced by gut bacteria during *in vitro* growth in pollen-conditioned medium. (A) Line graphs show growth of each community member in control medium and pollen-conditioned medium based on colony-forming unit (CFU) counts at time-point 0 h and 16 h. Values are the mean of five replicates with error bars indicating standard deviation. n.s = not significant, * = $p < 0.01$, ** = $p < 0.001$, $p < 0.0001$ = *** (Welch t-test). Volcano plots of significance (Welch t-test BH adj. *P*-value) vs. log2(fold change) show metabolic changes in pollen-conditioned medium at time-point 16 h relative to 0 h. Ions identified as pollen-derived are highlighted in black. Ions annotated as glycosylated flavonoids, flavonoid aglycones (non-glycosylated flavonoids), or putative flavonoid breakdown products are shown

1061   in color when they displayed log2(fold changes) ≥|1|. Other annotated ions are

1062   plotted in grey. (B) Model for the metabolism of flavonoids in the bee gut.

1063   Flavonoids are deglycosylated by specific bee gut bacteria resulting in the

1064   release of flavonoid aglycones. The sugar residues are likely fermented into

1065   organic acids. Accumulation of several (poly)phenol breakdown products *in vivo*

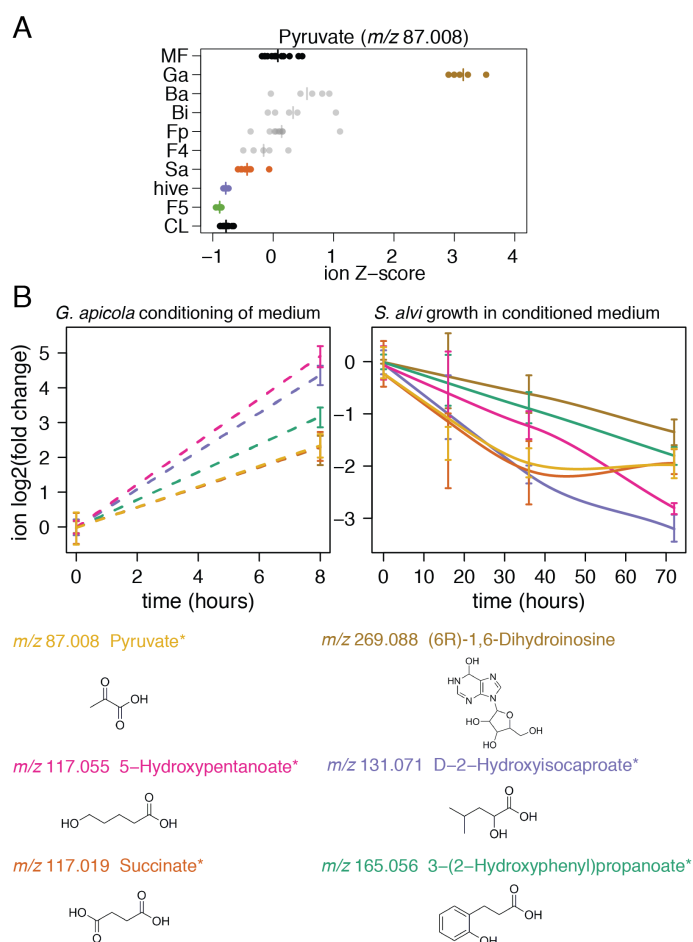1066   and *in vitro* suggests that the aglycone may be broken down further.

1067

1068

1069

1070 **Figure 6. Cross-feeding between *G. apicola* and *S. alvi*.** (A) Evidence for cross-

1071 feeding of pyruvate in the honey bee gut. Z-score transformed ion intensities

1072 reveal that the ion annotated as pyruvate accumulates in bees mono-colonized

1073 with *G. apicola*, but is depleted in hive bees, CL bees, and bees mono-colonized

1074 with *S. alvi* and Firm-5. (B) Six potentially cross-fed ions which accumulated

1075 during *in vitro* growth of *G. apicola* (left sub-panel) and were consumed by *S. alvi*

1076 when it was grown on the *G. apicola*-conditioned medium mixed 1:1 with fresh

1077 medium (right sub-panel). Smoothed lines are added for interpretation purposes

1078 only and are dashed in the left panel because they are drawn through two points

1079 only. Error bars represent the standard deviation based on three replicate

1080   cultures. Chemical structures of the first annotation of each ion are shown.

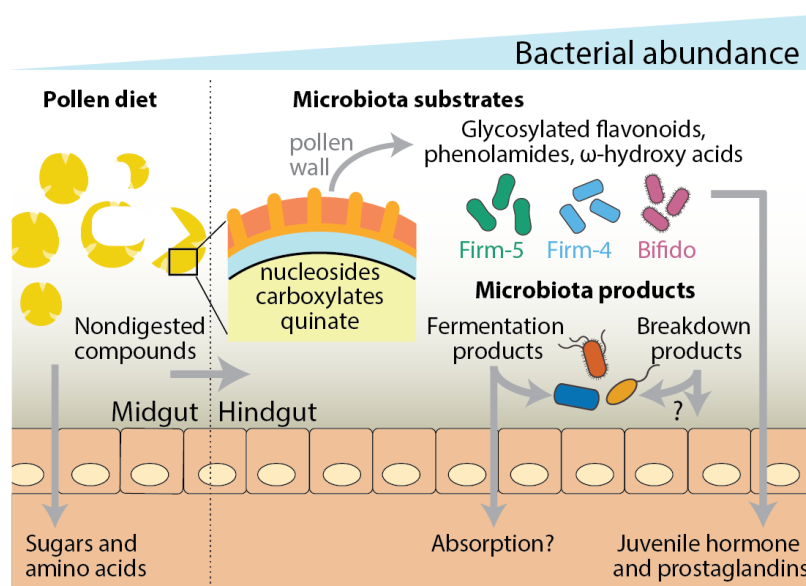1081   Asterisks indicate ions with ambiguous annotations.

1082

1083

1084

Figure 7. A summary of the metabolic activities of the bee gut microbiota identified in this study. Pollen is likely predigested in the midgut where bacterial levels are relatively low [45]. Here, the host absorbs accessible pollen-derived compounds such as simple sugars (glucose or fructose) and amino acids [46,47]. Non-digested pollen grains and pollen compounds enter the hindgut where bacterial density is much higher. We found nucleosides, various carboxylic acids (e.g. citrate, malate, fumarate) and aromatic compounds (such as quinate) from pollen to be utilized by bee gut bacteria. In the posterior part of the hindgut, three community members (Firm-5, Firm-4, and *B. asteroides*) metabolize major components of the outer pollen wall, including flavonoids, phenolamides and ω-hydroxy acids. The metabolic activities of the microbiota lead to the accumulation of fermentation products and intermediates of aromatic compound degradation. Some of the bacterial products may be utilized by other community members, as exemplified by the cross-feeding between *G. apicola* and *S. alvi,* or absorbed by the host. In addition, the gut symbiont *B. asteroides* seems

1100   to increase the production of several host metabolites (juvenile hormone

1101   derivatives and prostaglandins) that have key functions in immunity and

1102   physiology.